Original Article

Neuroprotective effect of *Paeoniae Radix Rubra* on hippocampal CA1 region of mice induced by transient focal cerebral ischemia via anti-gliosis and anti-oxidant activity

Xiao-lu Zhu [a,d,1], Bing-chun Yan [a,b,c,1], Cheng Tang [a], Guo-wei Qiu [a], Yao Wu [a], Jie Wang [a], Ping Bo [a,*]

[a] *Department of Traditional Chinese and Western Medicine, Jiangsu Key Laboratory of Integrated Traditional Chinese and Western Medicine for Prevention and Treatment of Senile Diseases, Yangzhou University, Yangzhou 225001, China*
[b] *Department of Neurology, Affiliated Hospital, Yangzhou University, Yangzhou 225001, China*
[c] *Jiangsu Key Laboratory of Zoonosis, Jiangsu Co-innovation Center for Prevention and Control of Important Animal Infectious Diseases and Zoonoses, Yangzhou University, Yangzhou 225009, China*
[d] *Medical Center, Yangzhou University, Yangzhou 225001, China*

ARTICLE INFO

ABSTRACT

Objective: Stroke is the second leading cause of death worldwide. This study aimed to investigate the neuroprotective effect of *Paeonia Radix Rubra* (PRR) on ischemic stroke of mice.
Methods: The focal ischemic stroke model was produced via middle cerebral artery occlusion. The experimental mice were divided into four groups: vehicle-sham group, PRR-sham group, vehicle-ischemia group, and PRR-treated ischemia group. The cerebral infarction volume was detected with TTC staining. The number of neurons in the hippocampal CA1 of the ischemic side, and the activation of astrocytes and microglia were observed via immunohistochemical staining. Western blotting was used to determine the expression changes of SOD1, SOD2, and Catalase protein levels in the hippocampus.
Results: PRR significantly reduced the cerebral infarct volume induced by ischemic injury and inhibited the astrocytes and microglia activation in the hippocampal CA1 region. The decreased levels of SOD1, SOD2, and Catalase that was induced by ischemic reperfusion were simultaneously improved after PRR treatment.
Conclusion: PRR improved neuronal injuries that were induced by transient cerebral ischemia via inhibiting gliosis and elevating anti-oxidants.

© 2018 Tianjin Press of Chinese Herbal Medicines. Published by Elsevier B.V. All rights reserved.

1. Introduction

Stroke is a class of acute cerebrovascular diseases that include cerebral hemorrhage, cerebral infarction, and subarachnoid hemorrhage that are manifested as focal or diffused brain dysfunction (Jin, Di Legge, Ostbye, Feightner, & Hachinski, 2006). Stroke is a major disease that contributes to a high mortality, disability, and morbidity (Go et al., 2014; Powers et al., 2015). Stroke is not only the second leading cause of death worldwide, but are also the third most common cause of disability (Endres, Heuschmann, Laufs, & Hakim, 2011; Feigin et al., 2014; Yang et al., 2013). It is estimated that 16.9 million cases of incident stroke were reported in 2010 (Feigin et al., 2014). Stroke is divided into either ischemic or hemorrhagic stroke. Ischemic stroke accounts for 87% of all stroke (Saada et al., 2014). Previous research has reported that various mechanisms are related to ischemic stroke such as excitotoxicity, oxidative stress, and inflammation (Gupta, Sharma, Jagannathan, & Gupta, 2017).

Paeoniae Radix Rubra (PRR) is the dried root of *Paeonia lactiflora* Pall. and *Paeonia veitchii* Lynch. PRR is a herbal medicine, containing paeony total glucosides, tannins, flavones, and volatile oil (Lu et al., 2015). Meanwhile, paeoniflorin, a bioactive monoterpene glucoside, is a major component existing in PRR (Wang et al., 2008). PRR is extensive used in traditional Chinese medicine for the treatment of blood-heat and blood-stasis syndrome (Huang et al., 2016). Xie et al reported that PRR significantly regulated microcirculation, improved hemodynamics, and inhibited the formation of thrombosis by modulating the active substances in the vascular endothelium, promoting blood flow, and anticoagulation (Xie, Cui, Shan, & Kang, 2017). The combination of

---

Ligusticum chuanxiong and PRR could inhibit neuronal apoptosis by attenuating ER-stress-dependent apoptotic signaling and protecting the blood-brain barrier (Gu et al., 2016). It has been reported that PRR might protect hippocampal CA1 neuron through suppressing the increase of intracellular Na^+ concentration (Dong et al., 2002). However, PRR plays its neuroprotective role in the transient focal ischemia induced by middle cerebral artery occlusion (MCAO), which is not yet reported. Therefore, in this study, we observed the neuroprotective effect of PRR on the focal cerebral ischemia of mice. Moreover, we also observed the changes of gliosis and oxidative stress after the pretreatment of PRR to explore the mechanism of its neuroprotection.

2. Materials and methods

2.1. Experimental animals

The progeny of male Institute of Cancer Research (ICR) mice [B.W., (25–30) g; 8 weeks of age] were purchased from the Comparative Medicine Center of Yangzhou University (Yangzhou, China), and used after one week of acclimation. They were housed in a conventional state under adequate temperature (23 ± 3) °C and relative humidity $(55 \pm 5)\%$ control with a 12 h light/12 h dark cycle, and free access to food and water. All experimental procedures conformed to the National Institutes of Health guidelines for the care and use of laboratory animals. All experiments were made to minimize the number of animals used and the suffering caused by the procedures used in the study. The animal protocol was approved based on ethical procedures and scientific care by the Yangzhou University—Institutional Animal Care and Use Committee (YIACUC-14-0014).

2.2. Drug treatment

The animals were divided into four groups ($n = 10$ in each group): vehicle-sham group (0.9% saline-treated group), PRR-sham group (25 mg/kg PRR-treated sham group, vehicle-ischemia group (0.09% saline-treated ischemia group), and PRR-treated ischemia group (25 mg/kg PRR-treated ischemia group). The PRR were administered by gavage 3 d before MCAO. The sham group and ischemia group were given with the same volume of 0.9% saline by gavage. PRR was purchased from Yangzhou Traditional Chinese Medical Hospital (Lot number 180305010).

2.3. Transient focal cerebral ischemia

The focal cerebral ischemia mice were introduced based on the method of Longa, Weinstein, Carlson, and Cummins (1989). Mice were initially anesthetized with 3.0% isoflurane (RWD, China) in a 67% N_2O and 33% O_2 mixture via face mask. Anesthesia was maintained with 2% isoflurane. Briefly, the left common carotid artery was exposed through a midline cervical incision. The left external carotid artery (ECA) was dissected free and isolated distally by coagulating its branches and placing a distal ligation. A piece of nylon suture was inserted into the lumen of right ECA stump and gently advanced 10 mm into the internal carotid artery (ICA) from the bifurcation to occlude the ostium of middle cerebral artery. After 1 h of ischemia, the suture was pulled back and the animals were allowed to recover. Sham-operated animals were subjected to the same surgical procedures such as separated on the neck muscles, blood vessels, except that the ICA was not inserted. A rectal temperature probe was introduced, and a heating pad maintained the body temperature at (37 ± 0.5) °C during whole surgery period. All the experimental animals were performed a neurobehavioral score and sacrificed 24 h after operation, and the corresponding tissues were prepared.

2.4. Neurobehavioral score

Longa scoring method was used to detect the extent of regional motor damage after cerebral ischemic reperfusion (Longa et al., 1989). The neurological examination was divided into five grades: 0 point: normal, no nerve function defect; 1 point: the left forepaw cannot stretch, mild neurological defect; 2 points: when walking, skewed to the left of the body, without dumping, moderate neurological deficit; 3 points: when walking, dumped to the left of the body, severe neurological deficit; 4 points: loss of consciousness. The score of 0 and 4 points in mice were excluded.

2.5. TTC staining and quantification of infarct volume

The mice were sacrificed with 4 mL/kg 10% chloral hydrate (Aladdin, Shanghai, China) 24 h after MCAO, and their brains were cut into coronal slices 2 mm thick using a mice brain matrix (RWD, China). The brain slices were then incubated in 2% 2,3,5-triphenyltetrazoliumchloride (TTC; Sigma, St. Louis, MO). After staining with 2% TTC for 0.5 h at room temperature in the dark, the brain slices were fixed with 4% formalin at room temperature overnight. The viable part of brain slice was red, while the infarct part was pale white. The infarct area and the whole area of each brain slice were measured with Image J. The infarct volume was calculated by multiplying the added infarct areas of each slices by slice thickness (2 mm), and results were expressed as the ratio of (infarct volume/whole brain volume) × 100%.

2.6. Tissue processing for histology

For the histological analysis, tissue sections were prepared from the sham- and MCAO-operated animals ($n = 5$ in each group). The animals were anesthetized with 4 mL/kg 10% chloral hydrate 24 h after surgery and perfused transcardially with 0.1 mol/L phosphate-buffered saline (PBS, pH 7.4) followed by 4% paraformaldehyde in 0.1 mol/L phosphate buffer (PB, pH 7.4). The brains were removed and postfixed in the same fixative for 6 h. The brain tissues were cryoprotected by infiltration with 30% sucrose overnight. The brain tissues were serially sectioned on a cryostat (Leica, Wetzlar, Germany) into 30 μm coronal sections and collected into six-well plates.

2.7. Immunohistochemistry

To examine neuronal damage and gliosis in the mouse hippocampal CA1 region after MCAO, antibody NeuN (a marker for neuron) immunohistochemistry was performed according to the method of the previous study (Yan, Park, et al., 2014). Meanwhile, antibody GFAP (glial fibrillary acidic protein) and Iba-1 were used to observe the activation of glial. In brief, the sections were sequentially treated with 0.3% hydrogen peroxide (H_2O_2) in PBS for 30 min and 10% normal serum in 0.05 mol/L PBS for 30 min. The sections were next incubated with diluted rabbit anti-NeuN (1:1000, CST, USA), rabbit anti-GFAP (1:500; Abcam, UK), goat anti-IBA-1 (1:500; Abcam, UK) overnight at 4 °C. Thereafter, the tissues were exposed to streptavidin peroxidase-conjugated biotinylated goat anti-rabbit IgG or rabbit anti-goat IgG (1:250, Vector, Burlingame, CA), after which they were visualized with 3,3′-diaminobenzidine (Sigma-Aldrich, St. Louis, MO, USA) in 0.01 mol/L PBS and mounted on Adhesion Microscope slides. Following dehydration, the tissue sections were mounted with neutral balsam (Solarbio, Beijing, China). To evaluate neuronal damage after MCAO, digital images of the hippocampus were captured with a computer-based microscope (Nikon, Chiyoda-Ku, Tokyo, Japan).

NeuN-immunoreactive neurons were counted in a $250 \times 250\,\mu m$ square applied approximately at the center of the hippocampal CA1 region using an image analyzing system (software Optimas 6.5; CyberMetrics, Scottsdale, AZ, USA). The studied tissue sections were selected with a $300\,\mu m$ interval, and cell counts were obtained by averaging the counts from each mouse. On the other hand, the staining intensity of GFAP, Iba1 immunoreactive structures was evaluated on the basis of an optical density (OD), which was obtained after the transformation of the mean gray level using the formula: $OD = \log (256/mean\ gray\ level)$. The OD of background was taken from areas adjacent to the measured area. After the background density was subtracted, a ratio of the OD of image file was calibrated as % (relative OD, ROD) using Adobe Photoshop version 8.0 and then analyzed using NIH Image 1.59 Software. All measurements were performed in order to ensure the objectivity in blind conditions, by two observers for each experiment, carrying out the measures of experimental samples under the same conditions.

2.8. Determination of malondialdehyde (MDA) content

MDA content was determined according to Malondialdehyde (MDA) Assay Kit (Jiancheng, Nanjing, China). The hippocampus was harvested after sacrificing. The tissues were disrupted via a crusher and centrifuged at 3500 rpm at 4 °C for 10 min. Then the supernatant was taken and incubated with pre-prepared MDA dye in boiling water for 15 min. The MDA content was determined by measuring the optical absorbance at 532 nm with a Microplate Reader. The experiment was performed in triplicate.

2.9. Western blot analysis

The experimental animals ($n = 5$ in each group) were used for Western blot analysis, as previously described (Yan, Ohk, et al., 2014). After sacrificing and removing the brains, they were serially and transversely cut into a thickness of $400\,\mu m$ on a vibratome, and the hippocampus was dissected with a surgical blade. Samples were preprocessed by Total Protein Extraction Kit (KeyGEN, Nanjing, China). Protein concentrations were determined using a Pierce BCA Protein Assay Kit (Thermo Scientific, USA). Equal amounts of total protein ($30\,\mu g$) were separated by 10% sodium dodecyl sulfate polyacrylamide gel electrophoresis (SDS-PAGE) and transferred to nitrocellulose membranes (Millipore, Bedford, MA, USA). In order to incubate antibodies, the same nitrocellulose membranes striped were used. In order to reduce background staining, the membranes were incubated with 5% BSA in TBS containing 0.1% Tween 20 for 60 min, followed by incubation with rabbit anti-SOD1 and 2 (1:1000, Abcam, UK), Catalase (1:1000, Abcam, UK), and β-actin (1:3000, Arigo, Taiwan, China) overnight at 4°C and subsequently exposed to secondary goat anti-rabbit IgG (1:5000, Santa Cruz, USA) for 2 h at room temperature, and the SuperSignal West Pico Chemiluminescent Substrate (Thermo Scientific, Rockford, USA) was used for protein detection. The result of western blot analysis was scanned, and densitometry analysis for the quantification of the bands was done using Quantity One Analysis Software (Bio-Rad), which was used to count relative optical density (ROD): A ratio of the ROD was calibrated as %, with sham group designated as 100%. Each blot shown was a representative of at least three similar independent experiments.

2.10. Statistical analysis

The data shown here represent the mean ± SEM. Differences of the means among the groups were statistically analyzed by a two-way analysis of variance followed by a post-Dunnett's test with

SPSS 19.0 Software (SPSS Inc., Chicago, IL, USA) to elucidate differences among the groups. Statistical significance was considered at $P < 0.05$.

3. Results

3.1. Score of neurological function

We evaluated the neurological function of the rats according to the longa scale (0–3). The mice in the PRR-ischemia group obtained better scores (neurological function of 1), than those in the MCAO group (neurological function of 3) (Fig. 1). These results indicated that PRR treatment ameliorated the neurological deficits of mice after ischemic reperfusion (IR).

3.2. Infract volume

We used Tetrazolium chloride (TTC) staining to evaluate the infract volume after IR. As shown in Fig. 2, in the group pretreated with PRR (PRR-treated ischemia group), the sizes of the infarcts (approximately 10% of the brain volume) were significantly decreased compared to those of the vehicle-ischemia group (approximately 42% of the brain volume).
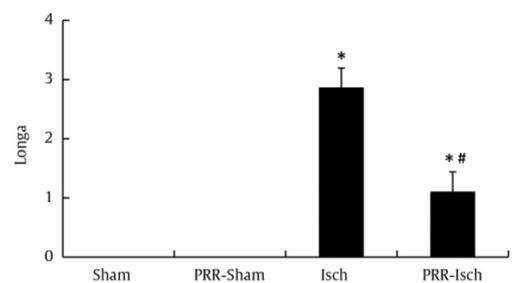

Fig. 1. Neurological function score in vehicle-sham group, PRR-sham group, vehicle-ischemia group, and PRR-treated ischemia group ($n = 10$). *$P < 0.05$ vs vehicle-sham group; #$P < 0.05$ vs vehicle-ischemia group.
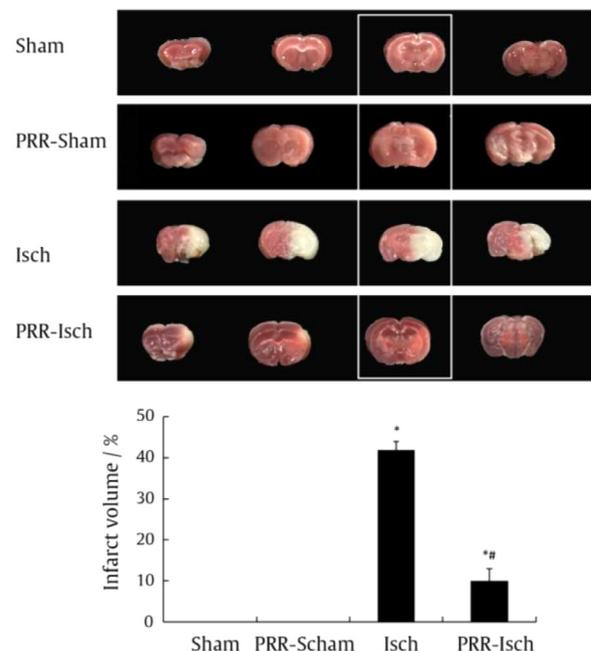

Fig. 2. Infract volume in vehicle-sham group, PRR-sham group, vehicle-ischemia group, and PRR-treated ischemia group ($n = 5$). *$P < 0.05$ vs vehicle-sham group; #$P < 0.05$ vs vehicle-ischemia group.

3.3. Effect of PRR on NeuN immuohistochemistry in hippocampus CA1 region

NeuN immunohistochemistry was used to examine the neuroprotective effects of PRR on neuron in the hippocampus CA1 region. As shown in Fig. 3, NeuN-positive (+) neurons were easily observed in the cerebral cortex and showed no significant differences in each sham groups. The NeuN$^+$ neurons in the hippocampus CA1 region of vehicle-ischemia group decreased significantly (about 17% of those in the sham groups). However, the number of NeuN-positive (+) neurons in the CA1 region after pretreatment with PRR was significantly increased compared to those in the vehicle-ischemia group.

3.4. Effect of PRR on activation of glial in hippocampus CA1 region

3.4.1. GFAP immunoreactivity

The changes of astrocytes activation in the ischemic CA1 region of mice were examined by glial fibrillary acidic protein (GFAP) immunohistochemistry. As shown in Fig. 4, in each sham groups, GFAP$^+$ astrocytes showed a rest form and distributed in all the layers of the CA1 region. In the vehicle-ischemia group, the GFAP$^+$astrocytes were larger than those in the sham groups, and their GFAP immunoreactivity was increased. However, the immunoreactivity of GFAP decreased markedly after treatment of PRR and the morphology of the GFAP$^+$ astrocytes were similar to the vehicle-sham group.

3.4.2. Iba-1 immunoreactivity

The changes of microglia activation in the ischemic CA1 region of mice were examined by ionized calcium-binding adapter molecule (Iba-1) immunohistochemistry. As shown in Fig. 5, in each sham group, we did not find any activated Iba-1$^+$ microglia in the CA1 region. In the vehicle-ischemia group, Iba-1$^+$ microglia

were larger in size, and their Iba-1immunoreactivity significantly increased compared to those in the sham groups. However, the immunoreactivity of Iba-1 decreased markedly after treatment of PRR and the morphology of the Iba-1$^+$ microglia were similar to the vehicle-sham group.

3.5. Effect of PRR on level of reactive oxygen species in hippocampus

The levels of reactive oxygen species in the hippocampus were examined by measuring the level of MDA. As shown in Fig. 6A, we found that the level of MDA increased markedly in the ischemia group compared to those in the sham group. Moreover, we found that the level of MDA decreased significantly in the PRR-treated ischemia group compared to those in the ischemia group.

3.6. Effect of PRR on expression of SOD1, SOD2, and catalase in hippocampus CA1 region

The levels of SOD1, SOD2, and Catalase in the hippocampus were examined by western blot analysis. As showed in Fig. 6, we found that the protein levels of SOD1, SOD2, and Catalase decreased markedly in the vehicle-ischemia group compared to those in the vehicle-sham group. Moreover, we found that the protein levels of the above mentioned antioxidant enzymes were increased significantly in the PRR-treated ischemia group compared to those in the vehicle-ischemia group (Fig. 6B and C).

4. Discussion

The PRR, a Chinese materia medica (CMM), plays an important role in the clinic treatment of blood stasis in China (Xie et al., 2017). PRR is commonly used to reduce fever, cool blood, eliminate blood stasis, activate blood circulation, and relieve
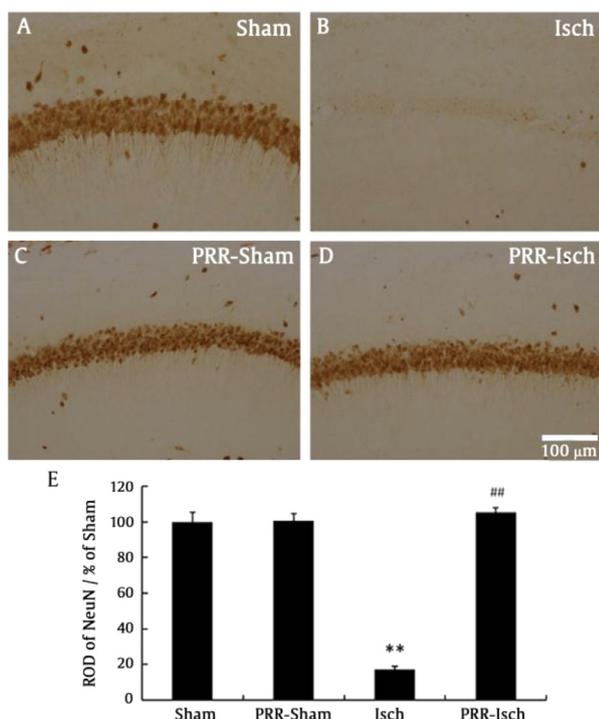

Fig. 3. NeuN immunoreactivities in hippocampal CA1 region of vehicle-sham group, PRR-sham group, vehicle-ischemia group, and PRR-treated ischemia group ($n = 5$, Scale bar = 100 μm). $^{**}P < 0.01$ *vs* vehicle-sham group; $^{##}P < 0.01$ *vs* vehicle-ischemia group.
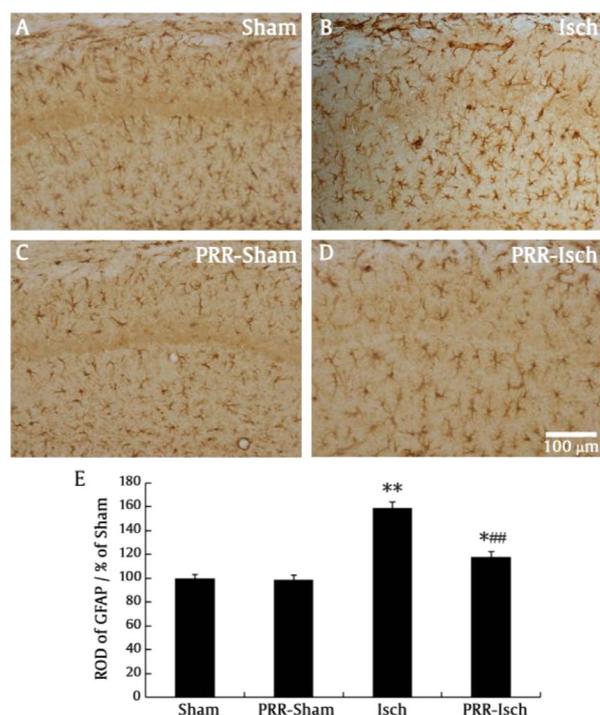

Fig. 4. GFAP immunoreactivity in hippocampal CA1 region of vehicle-sham group, PRR-sham group, vehicle-ischemia group and PRR-treated ischemia group ($n = 5$, Scale bar = 100 μm). $^{**}P < 0.01$ *vs* vehicle-sham group; $^{##}P < 0.01$ *vs* vehicle-ischemia group.
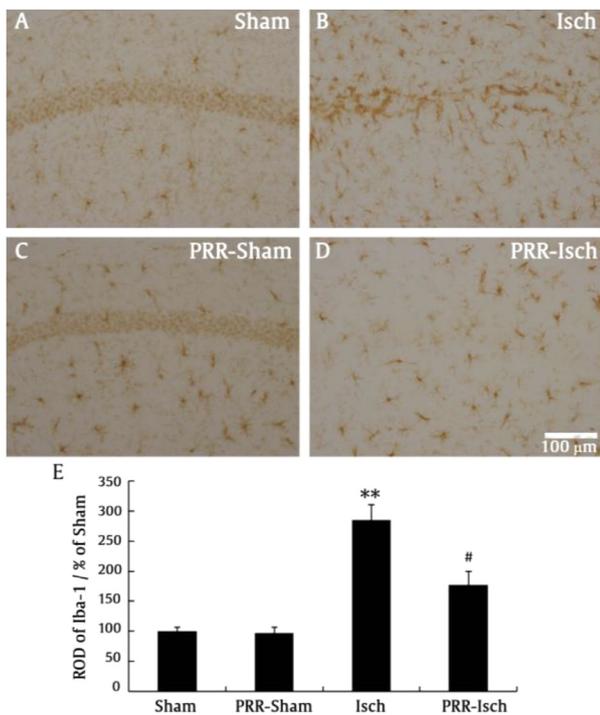
Fig. 5. Iba-1 immunoreactivity in hippocampal CA1 region of vehicle-sham group, PRR-sham group, vehicle-ischemia group, and PRR-treated ischemia group ($n = 5$, Scale bar = 100 μm). $**P < 0.01$ vs vehicle-sham group; $#P < 0.05$ vs vehicle-ischemia group.

pain (Zhan et al., 2017). There are various biological activities of the compounds or extracts from PRR, including anti-oxidant, antithrombotic, anti-inflammation, and free radical scavenging activities (Lee, Kwon, Son, Kim, & Heo, 2005; Tang, Liu, Hsieh, & Hsieh, 2010). We confirmed the neuroprotective effect of PRR on protecting the neuronal damage in mice induced by focal transient ischemia. Our results were supported by previous studies, which showed that PRR could inhibit neuronal apoptosis by attenuating the ER-stress-dependent apoptotic signaling and protecting the blood-brain barrier (Gu et al., 2016).

The mechanism of cerebral ischemic reperfusion (IR) injury is significantly complex, including excitotoxicity, oxidative stress, the response of inflammatory mediators, and apoptosis (Ashafaq et al., 2012; Yaidikar et al., 2015). Microglia and astrocytes are resident immunocytes in the central nervous system, where they play important roles in the inflammatory response (Farina, Aloisi, & Meinl, 2007). Many researchers have reported the change in GFAP and Iba-1 immunoreactivity in the ischemic CA1 region was associated with neuronal death (Yan, Ohk, et al., 2014). Gliosis

of astrocytes and microglia was easily induced in the hippocampus CA1 region after transient cerebral ischemia in the ICR mice, which were closely related to the response of inflammatory mediators induced by transient cerebral ischemia. Meanwhile, the acute inflammatory responses play an important role in cerebral ischemia reperfusion injury (Shichita, Ito, & Yoshimura, 2014). Microglia and astrocytes could produce pro-inflammatory cytokines, and then exacerbate the damage of neuron (Pekny, Wilhelmsson, & Pekna, 2014; Ransom et al., 2012). The death/damage of neuron was caused by the release of tumor necrosis factor alpha (TNF-α) and interleukin-1 (IL-1) after the activation of microglia and astrocytes (Shichita et al., 2014). The inflammation occurs early in the hippocampus, cortex or other region after cerebral ischemia, because of the activation, aggregation, and infiltration of glial cells. In this study, the immunoreactivity of GFAP and Iba-1 significantly increased in the hippocampus CA1 region after 24 h IR. However, the immunoreactivity of GFAP and Iba-1 decreased markedly after treatment of PRR. These results demonstrated that the neuroprotective effect of PRR was related to the inhibition of gliosis after IR.

Oxidative stress plays a very important role in brain injury induced by IR (Sharma et al., 2014; Shichita et al., 2014; Wakayama, Shimamura, Suzuki, Watanabe, & Koriyama, 2017). A great number of researches have reported that the accumulation of reactive oxygen species (ROS) is produced during cerebral IR, which cause the oxidation of lipids, proteins, and DNA and subsequently cellular damage and apoptosis (Jia, Han, Yang, & Zhao, 2014; Wong et al., 2008). Furthermore, free radicals actively attack macromolecules within glial cells, resulting in astrocytes and microglia respond to the oxidative insult by gliosis, and then aggravate the damage of neuron (Baydas, Sonkaya, Tuzcu, Yasar, & Donder, 2005). The endogenous antioxidant defense mechanisms via the function of the SODs and Catalase play an important role in the reduction and elimination of free radicals (Yaidikar & Thakur, 2015). During I/R injury, excessively generated ROS induced by I/R cannot be efficiently removed by the endogenous antioxidant systems, and a burst of ROS lead to brain dysfunction and cell death (Jia et al., 2014; Oliver et al., 1990). Therefore, many researches have reported that various antioxidants or drugs with antioxidant capacity could improve the neuronal damage induced by ROS after cerebral IR. In this study, the expression levels of SOD1, SOD2, and Catalase were increased after treatment with the PRR compared to those in the vehicle-ischemia group. These results suggested that the PRR could increase significantly the levels of endogenous antioxidant enzymes to decrease the accumulation of ROS, and then improve gliosis and the neuronal damage in the hippocampus CA1 region.

In conclusion, PRR could improve the injury of neurologic function and neuronal survival against transient cerebral IR. Moreover, its effect on inhibition of gliosis and increasing of anti-oxidant were closely related to the function of neuroprotection.
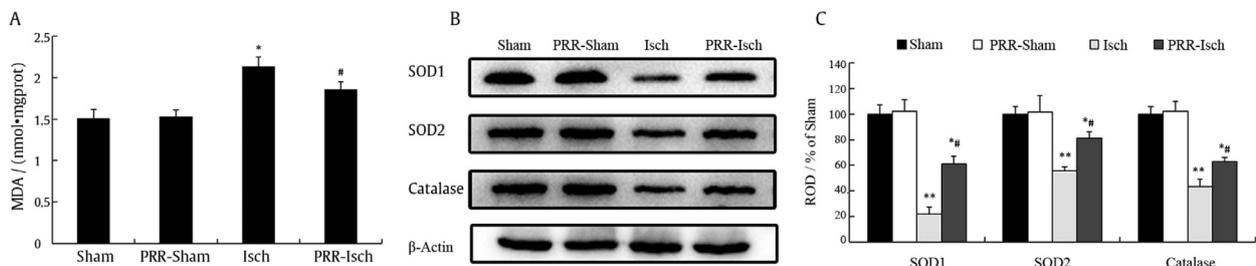

Fig. 6. Levels of MDA in hippocampal of vehicle-sham group, PRR-sham group, vehicle-ischemia group, and PRR-treated ischemia group (A), Western blot analysis of SOD1, SOD2, and Catalase in hippocampal (B and C), ROD as a percentage of immunoblot band was presented ($n = 5$). $*P < 0.05$, $**P < 0.01$ vs vehicle-sham group; $#P < 0.05$ vs vehicle-ischemia group. *Bars* indicate mean ± SD.

Conflict of interest

Acknowledgments

References

Ashafaq, M., Khan, M. M., Shadab, Raza S., Ahmad, A., Khuwaja, G., Javed, H., et al. (2012). S-allyl cysteine mitigates oxidative damage and improves neurologic deficit in a rat model of focal cerebral ischemia. *Nutrition Research, 32*, 133–143.

Baydas, G., Sonkaya, E., Tuzcu, M., Yasar, A., & Donder, E. (2005). Novel role for gabapentin in neuroprotection of central nervous system in streptozotocine-induced diabetic rats. *Acta Pharmacologica Sinica, 26*, 417–422.

Dong, X. P., & Xu, T. L. (2002). *Radix Paeoniae Rubra* suppression of sodium current in acutely dissociated rat hippocampal CA1 neurons. *Brain Research, 940*, 1–9.

Endres, M., Heuschmann, P. U., Laufs, U., & Hakim, A. M. (2011). Primary prevention of stroke: Blood pressure, lipids, and heart failure. *European Heart Journal, 32*, 545–552.

Farina, C., Aloisi, F., & Meinl, E. (2007). Astrocytes are active players in cerebral innate immunity. *Trends Immunology, 28*, 138–145.

Feigin, V. L., Forouzanfar, M. H., Krishnamurthi, R., Mensah, G. A., Connor, M., Bennett, D. A., et al. (2014). Global and regional burden of stroke during 1990--2010: Findings from the global burden of disease study 2010. *The Lancet, 383*, 245–254.

Go, A. S., Mozaffarian, D., Roger, V. L., Benjamin, E. J., Berry, J. D., Blaha, M. J., et al. (2014). American heart association statistics C, stroke statistics S, 2014. Heart disease and stroke statistics—2014 update: A report from the American heart association. *Circulation, 129*, e28–e292.

Gu, J., Chen, J., Yang, N., Hou, X., Wang, J., Tan, X., et al. (2016). Combination of Ligusticum chuanxiong and *Radix Paeoniae* ameliorate focal cerebral ischemic in MCAO rats via endoplasmic reticulum stress-dependent apoptotic signaling pathway. *Journal of Ethnopharmacology, 187*, 313–324.

Gupta, S., Sharma, U., Jagannathan, N. R., & Gupta, Y. K. (2017). Neuroprotective effect of lercanidipine in middle cerebral artery occlusion model of stroke in rats. *Experimental Neurology, 288*, 25–37.

Huang, Y. Q., Ma, X., Wang, J., Zhao, Y. L., Wang, J. B., & Chen, Z. (2016). Therapeutic efficacy and safety of *Paeoniae Radix Rubra* Formulae in relieving Hyperbilirubinemia induced by Viral Hepatitis: A meta-analysis. *Frontiers in Pharmacology, 7*, 63.

Jia, D., Han, B., Yang, S., & Zhao, J. (2014). Anemonin alleviates nerve injury after cerebral ischemia and reperfusion (i/r) in rats by improving antioxidant activities and inhibiting apoptosis pathway. *Journal of Molecular Neuroscience, 53*, 271–279.

Jin, Y. P., Di Legge, S., Ostbye, T., Feightner, J. W., & Hachinski, V. (2006). The reciprocal risks of stroke and cognitive impairment in an elderly population. *Alzheimers & Dementia, 2*, 171–178.

Lee, S. C., Kwon, Y. S., Son, K. H., Kim, H. P., & Heo, M. Y. (2005). Antioxidative constituents from *Paeonia lactiflora*. *Archives of Pharmacal Research, 28*, 775–783.

Longa, E. Z., Weinstein, P. R., Carlson, S., & Cummins, R. (1989). Reversible middle cerebral artery occlusion without craniectomy in rats. *Stroke, 20*, 84–91.

Lu, X. H., Ma, X., Wang, J., Zhu, Y., Zhou, Z. Y., & Chen, Z. (2015). Research progress on chemical constituents of *Paeoniae Rubra Radix* and their pharmacological effects. *Chinese Herbal Medicines, 46*(4), 595–602.

Oliver, C. N., Starke-Reed, P. E., Stadtman, E. R., Liu, G. J., Carney, J. M., & Floyd, R. A. (1990). Oxidative damage to brain proteins, loss of glutamine synthetase activity, and production of free radicals during ischemia/reperfusion-induced injury to gerbil brain. *Proceedings of the National Academy of Science of the United States of America., 87*, 5144–5147.

Pekny, M., Wilhelmsson, U., & Pekna, M. (2014). The dual role of astrocyte activation and reactive gliosis. *Neuroscience Letters, 565*, 30–38.

Powers, W. J., Derdeyn, C. P., Biller, J., Coffey, C. S., Hoh, B. L., Jauch, E. C., et al. (2015). 2015 American heart association/American stroke association focused update of the 2013 guidelines for the early management of patients with acute ischemic stroke regarding endovascular treatment: A guideline for healthcare professionals from the American heart association/American stroke association. *Stroke, 46*, 3020–3035.

Ransom, B. R., & Ransom, C. B. (2012). Astrocytes: Multitalented stars of the central nervous system. *Methods in Molecular Biology, 814*, 3–7.

Saada, F., & Antonios, N. (2014). Existence of ipsilateral hemiparesis in ischemic and hemorrhagic stroke: Two case reports and review of the literature. *European Neurology, 71*, 25–31.

Sharma, T., Airao, V., Panara, N., Vaishnav, D., Ranpariya, V., Sheth, N., et al. (2014). Solasodine protects rat brain against ischemia/reperfusion injury through its antioxidant activity. *European Journal of Pharmacology, 725*, 40–46.

Shichita, T., Ito, M., & Yoshimura, A. (2014). Post-ischemic inflammation regulates neural damage and protection. *Frontiers in Cellular Neuroscience, 8*, 319.

Tang, N. Y., Liu, C. H., Hsieh, C. T., & Hsieh, C. L. (2010). The anti-inflammatory effect of *Paeoniflorin* on cerebral infarction induced by ischemia-reperfusion injury in Sprague-Dawley rats. *The American Journal of Chinese Medicine, 38*, 51–64.

Wakayama, K., Shimamura, M., Suzuki, J. I., Watanabe, R., Koriyama, H., et al. (2017). Angiotensin II peptide vaccine protects ischemic brain through reducing oxidative stress. *Stroke., 48*, 1362–1368.

Wang, C. H., Wang, R., Cheng, X. M., He, Y. Q., Wang, Z. T., & Wu, C. (2008). Comparative pharmacokinetic study of paeoniflorin after oral administration of decoction of *Radix Paeoniae Rubra* and *Radix Paeoniae Alba* in rats. *Journal of Ethnopharmacology, 117*, 467–472.

Wong, C. H., & Crack, P. J. (2008). Modulation of neuro-inflammation and vascular response by oxidative stress following cerebral ischemia-reperfusion injury. *Current Medicinal Chemistry, 15*, 1–14.

Xie, P., Cui, L., Shan, Y., & Kang, W. Y. (2017). Antithrombotic effect and mechanism of *Radix Paeoniae Rubra. BioMed Research International, 2017*, 9475074.

Yaidikar, L., & Thakur, S. (2015). Arjunolic acid, a pentacyclic triterpenoidal saponin of *Terminalia arjuna* bark protects neurons from oxidative stress associated damage in focal cerebral ischemia and reperfusion. *Pharmacological Reports, 67*, 890–895.

Yan, B. C., Ohk, T. G., Ahn, J. H., Park, J. H., Chen, B. H., Lee, J. C., et al. (2014). Differences in neuronal damage and gliosis in the hippocampus between young and adult gerbils induced by long duration of transient cerebral ischemia. *Journal of the Neurological Science, 337*, 129–136.

Yan, B. C., Park, J. H., Ahn, J. H., Kim, I. H., Park, O. K., Lee, J. C., et al. (2014). Neuroprotection of posttreatment with risperidone, an atypical antipsychotic drug, in rat and gerbil models of ischemic stroke and the maintenance of antioxidants in a gerbil model of ischemic stroke. *Journal of Neuroscience Research, 92*, 795–807.

Yang, G., Wang, Y., Zeng, Y., Gao, G. F., Liang, X., Zhou, M., et al. (2013). Rapid health transition in China, 1990–2010: Findings from the Global burden of disease study 2010. *The Lancet, 381*, 1987–2015.

Zhan, H., Fang, J., Tang, L., Yang, H., Li, H., Wang, Z., et al. (2017). Application of near-infrared spectroscopy for the rapid quality assessment of *Radix Paeoniae Rubra. Spectrochimica Acta Part A Molecular and Biomolecular Spectroscopy, 183*, 75–83.